Optical storage of orbital angular momentum via Rydberg electromagnetically induced transparency

Kai Wang (王 锴)[1,2,*], Wei Zhang (张 伟)[1,2], Zhiyuan Zhou (周志远)[1,2], Mingxing Dong (董明新)[1,2], Shuai Shi (施 帅)[1,2], Shilong Liu (刘世隆)[1,2], Dongsheng Ding (丁冬生)[1,2,], and Baosen Shi (史保森)[1,2]**

[1]*Key Laboratory of Quantum Information, CAS, University of Science and Technology of China, Hefei 230026, China*

[2]*Synergetic Innovation Center of Quantum Information and Quantum Physics, University of Science and Technology of China, Hefei 230026, China*

**Corresponding author: wkhy@ustc.edu.cn; **corresponding author: dds@ustc.edu.cn*

Received December 7, 2016; accepted February 24, 2017; posted online March 16, 2017

In this Letter, we report on the successful optical storage of orbital angular momentum (OAM) using Rydberg electromagnetically induced transparency (EIT) in cold rubidium atoms. With a storage time of 1.4 μs, the retrieved structure is highly similar, showing the ability of storing light's OAM at a principal quantum number of 20. The results at higher principal quantum numbers ($n = 25, 30$) are also measured. These results show the promise of image processing based on a Rydberg atomic system.

OCIS codes: 160.2900, 020.5780.
doi: 10.3788/COL201715.060201.

Photons are robust carriers of information, and memory for the state of light is a key step in the realization of long-distance communications. Many optical memories are based on light–atom interactions, such as electromagnetically induced transparency (EIT)[1,2], coherent population oscillation (CPO)[3,4], gradient echo memories[5], and the atomic frequency comb[6]. The combination of EIT and Rydberg atoms provides an effective interaction between photons. Such a process requires coherently mapping photonic states into and out of a Rydberg polariton on demand. Rydberg atoms are ideal for nonlinear interaction because of the strong dipole–dipole (DD) interaction between the Rydberg atoms[7–9]. The strong DD interaction leads to Rydberg blockade and can be used to implement a controlled-NOT gate[10], single-photon switches[11], transistors[12], and a controlled π phase shift[13].

Structured vortex beams with phase front $\exp(il\theta)$ carry an orbital angular momentum (OAM) of $l\hbar$ per photon[14–16], where l is a topological charge and θ represents an azimuthal angle. Photons with OAM could be regarded as helices with their left- and right-handedness twisted to varying degrees. Light encoded in OAM space could offer high channel capacity and also can provide capability for spatial manipulating[17]. Many groups and researchers have demonstrated the optical storage of OAM in atomic gas and solid matter systems[18–22].

The Rydberg interaction, which is dependent on the separation distance between the Rydberg atoms, creates an obstacle on subsequent excitations of neighboring ground state atoms. Such spatial dependent interaction could bring rich spatial dynamics behaviors, showing potential manipulation in image information processing. Moreover, exciting Rydberg atoms with OAM structure gives an additional degree of freedom for manipulating an image. Storing a structured vortex beams as a structured Rydberg collective excitation is a preliminary step.

In this Letter, we experimentally investigate the optical storage of OAM in cold rubidium atoms using the Rydberg EIT. We use a time-resolution camera to monitor the spatial structure of the probe beam carrying OAM before and after storage. The storage time could be up to 1.4 μs at a principal quantum number of 20. Higher principal numbers ($n = 25, 30$) are also given.

The experimental setup is similar to our previous device[23]: ^{85}Rb atoms are trapped in two-dimensional magneto-optical traps (MOTs); the atoms are prepared to the $5S_{1/2}$ (F = 2) state; the temperature of the atomic cloud is ~200 μK; the size is 2 mm × 2 mm × 30 mm; and, the optical depth of the cold atoms is 20. The experiment is run periodically with an MOT trapping time of 7.5 ms and an experiment operation time of 1.5 ms, which contains 300 cycles of Rydberg excitation operations. The probe laser is an external-cavity diode laser (DL100, Toptica), operating at a wavelength of 795 nm, which corresponds to the transition $5P_{1/2}$ (F = 2) → $5P_{1/2}$ (F = 3). The coupling laser is a frequency-doubled laser (SHG, Toptica) with an output power of 680 mW, operating at around 480 nm, which corresponds to the transition $5P_{1/2}$ (F = 3) → $nD_{3/2}$, shown in Fig. 1(a). The probe laser is locked via saturated absorption spectroscopy, the coupling laser is locked via two-photon dichroic atomic vapor laser locking (DAVLL). The probe and coupling beams collinearly counter-propagate through the MOT with the same horizontal linear polarization and are focused by a lens with a focal length of 200 mm to increase the interaction between the atoms and the laser. After the probe and coupling beams propagate through the cloud of

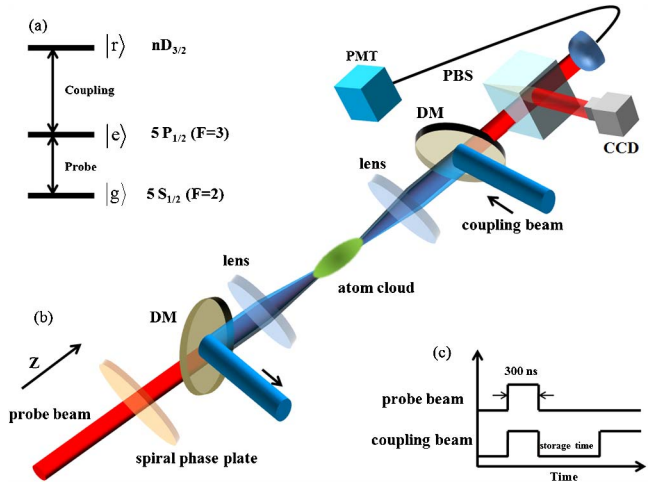

Fig. 1. (a) Atomic energy level diagram for Rydberg EIT. The probe laser couples the ground state, $|g\rangle = |S_{1/2}, F = 2\rangle$ with the excited state, $|e\rangle = |5P_{1/2}, F = 3\rangle$ the coupling laser couples the Rydberg excited states $|r\rangle$. (b) Simplified diagram of the optical beam path. The probe and coupling beams for the Rydberg EIT counter-propagate along the z axis. After propagating through the cloud of ^{85}Rb atoms, a DM splits off the coupling beam. A spiral phase plate is used for the probe beam so it carries a well-defined OAM of $2\hbar$. The probe beam is divided into two paths by a polarizing beam splitter (PBS) and detected on a PMT and a CCD. (c) Timing of the probe and coupling lasers.

^{85}Rb atoms, a dichroic mirror (DM) is used to split off the coupling beam. In the experiment, the power of coupling laser beam is 320 mW, with a beam waist of 20 μm. The probe beam has a beam waist of 18 μm. We insert a spiral phase plate (VPP-2, RPC Photonics, transmission coefficient 95%) in the optical path of the probe beam, therefore, the probe beam has a well-defined OAM of $2\hbar$. We use a photomultiplier tube (PMT) (H10721, Hamamatsu) to detect the intensities of probe field in the time domain and a time-resolution camera (CCD, 1024 × 1024, iStar 334T series, Andor) triggered by a synchronization signal generated by a signal generator (AFG 3252, Tektronix) to monitor its spatial structure. The schematic diagram is shown in Fig. 1(b). We switch the probe and coupling pulses on and off to realize Rydberg excitation and OAM storage; the timing sequence is shown in Fig. 1(c).

We first observe the EIT transmission by switching on the coupling laser, shown in Fig. 2(a); each data point has been averaged 16 times. The scan time of the probe laser is 50 μs, corresponding to the frequency range from −50 to 50 MHz. Since the probe beam has a donut-shaped structure [see Fig. 3(a)], its absorption width in the frequency domain is narrower than that in the Gaussian beam. The transparency peak in the spectrum is used to optimize the Rydberg excitation. The black line shows an EIT window with an FWHM of 5 MHz. The principal number of the Rydberg excitation is 20. For a larger principal number n (>30), the transition coefficient between the intermediate level and a high Rydberg level

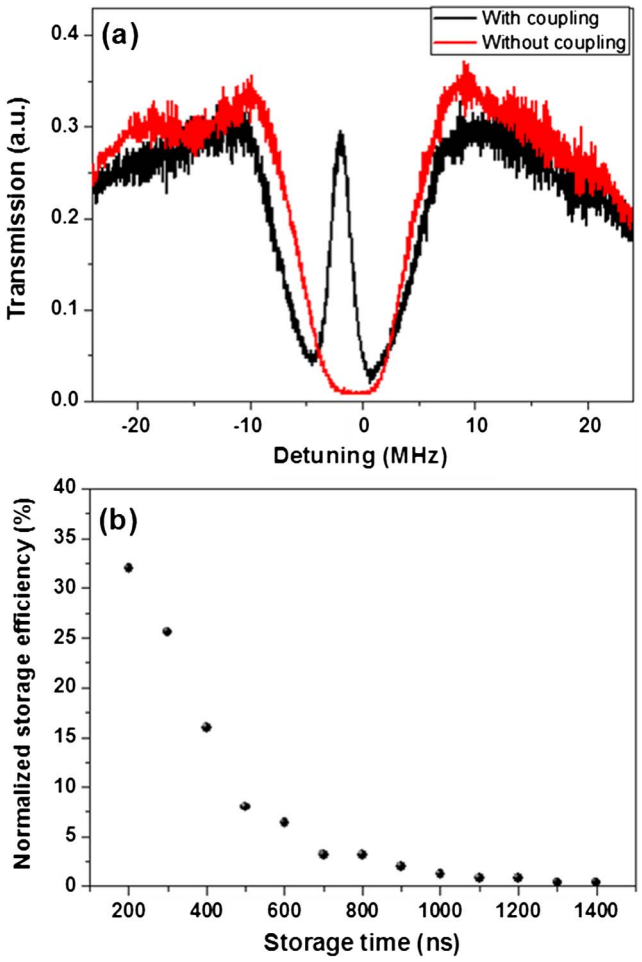

Fig. 2. (a) Transmission of the probe signal with (black) and without (red) coupling laser beam. (b) Storage efficiency as a function of storage time. The principal number of Rydberg excitation is 20.

is small; therefore, it needs a much higher power coupling laser.

We switch the probe and coupling pulses off to realize Rydberg excitation and OAM storage. Typical probe pulses have a temporal length of 300 ns; meanwhile, the coupling laser is on. Upon entrance into the atom cloud, the probe pulse is spatially compressed to zero due to reduced group velocity. Then, we turn off the coupling laser, and the probe pulse is stored in the Rb atoms while photons from the probe field are stored as Rydberg polaritons. After some time interval, we turn on the coupling laser again to release the stored polaritons to the probe laser. We consider the storage time as the duration that the coupling laser is switched off completely, which is limited by the atomic coherence lifetime. The storage efficiency is obtained from the ratio between the input and the retrieved probe laser fields. Figure 2(b) shows the storage efficiency as a function of storage time when the principal number of the Rydberg excitation is 20.

The input and retrieval images of the probe beam for various storage times (ranging from 200 to 1400 ns) are depicted in Fig. 3. The probe beam with a

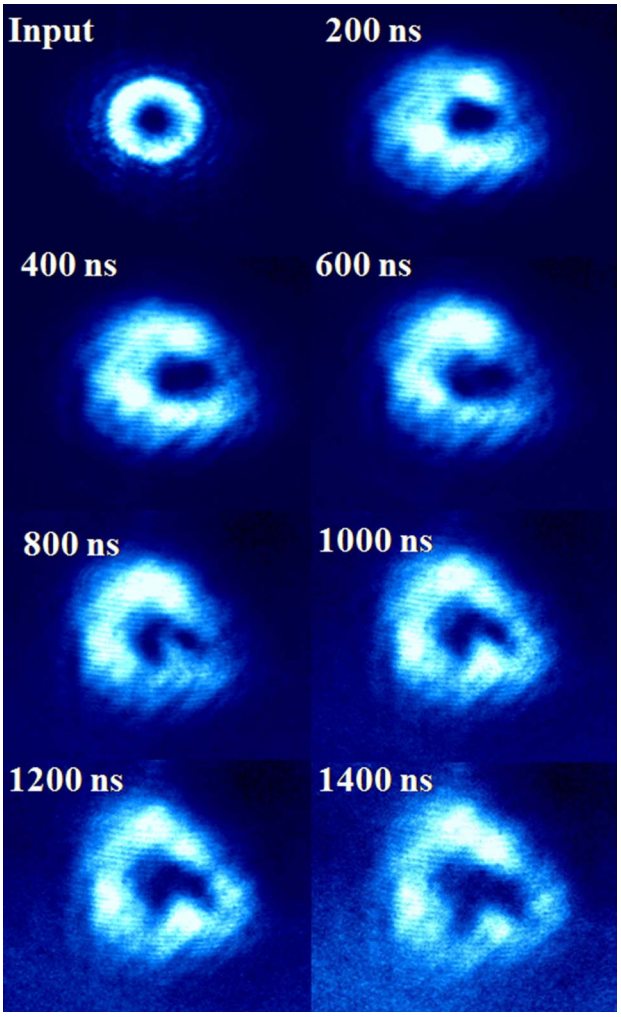

Fig. 3. Input and retrieval images of probe beam for various storages time at a principal quantum number of 20. Each image has the same dimensions and pixels. The central hole of the probe beam remains dark even for the longest storage time of 1400 ns.

Laguerre-Gauss (LG) mode has a helical structure. The electric field of the LG_0^l mode is given by $E_l(r,\theta) = A_l(r,w_0)e^{-il\theta}$ in polar coordinates of the $z=0$ plane[24], where w_0 is the waist, l is the topological charge, the radial cross section carrying a ring shaped is given by $A_l(r,w_0) = (\sqrt{2P/\pi l!}/w_0)(\sqrt{2}r/w_0)^l \exp(-r^2/w_0^2)$, where P is the total intensity. The LG mode carries OAM and has a $2\pi l$ phase twist around its dark center. The dark center of the light vortex can be described as a result of the phase singularity. In our experiment, $l=2$, and the image of the probe beam measured by the CCD when the coupling beam is off is shown in the upper left of Fig. 3. It is evident that the transverse mode of the probe beam increases as the storage time increases due to the effect of diffusion. We also note that the central hole of the helical beam remains dark even for the longest storage time of 1400 ns, which means there is a high topological stability for the stored OAM. Since diffusion is homogeneous and isotropic, atoms enter the dark center from all directions carrying a phase that is uniformly distributed over the unit circle; they destructively interfere, and thus the center of the probe beam maintains darkness. Therefore, vortex beams carrying OAM are ideal candidates for information storage due to their robustness to decoherence effects such as diffusion. The darkening of the retrieval image is mainly due to the slight noncoincidence of the pump optical paths. The deformation of the retrieval image is owing to the uneven distribution of the input light's intensity. These results exhibit the ability of Rydberg excitation to store the light with a vortex structure.

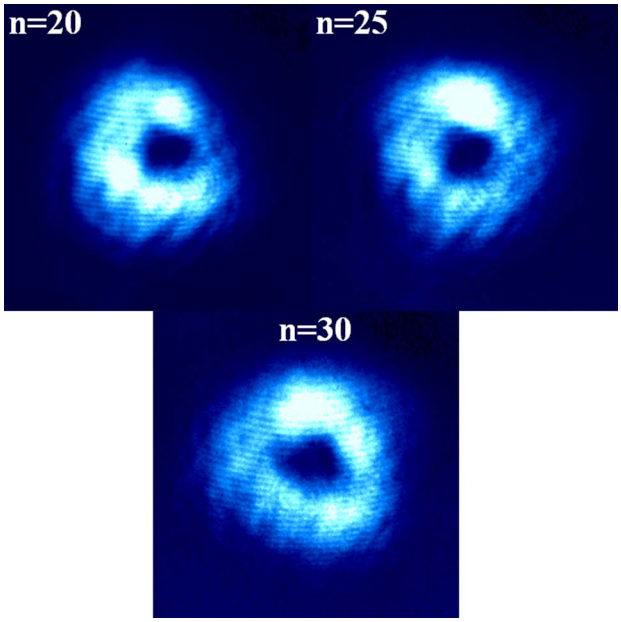

Fig. 4. Retrieval images of probe beam for various principal numbers of Rydberg excitation when the storage time is 300 ns.

We also measure the retrieval image of the probe beam at higher principal numbers ($n=25,30$) when the storage time is set to 300 ns. The results are similar in that the OAM could be stored, as shown in Fig. 4. The highest principal number of Rydberg excitation is 30 in our experiment, thus the blockade radius is too small to observe the blockade effect at present. We need a much stronger power for the coupling laser or a larger atomic density to perform the blockade effect.

In conclusion, we implement the optical storage of OAM in cold rubidium atoms using Rydberg EIT. The storage time can be up to 1.4 μs at a principal quantum number of 20. These results show the ability of Rydberg excitation to store the light with a vortex structure. In the future, we plan to perform Rydberg excitation with a larger principal number, n, in order to study blockade effects.

This work was supported by the National Fundamental Research Program of China (No. 2 011CBA00200), the National Natural Science Foundation of China (Nos. 11174271, 61275115, 61435011, and 61525504), and the Fundamental Research Funds for the Central Universities.

References

1. D. F. Phillips, A. Fleischhauer, A. Mair, and R. L. Walsworth, Phys. Rev. Lett. **86**, 783 (2001).
2. S. C. Zhang, S. Y. Zhou, M. M. T. Loy, G. K. L. Wong, and S. W. Du, Opt. Lett. **36**, 4530 (2011).
3. M. A. Maynard, F. Bretenaker, and F. Goldfarb, Phys. Rev. A **90**, 061801 (2014).
4. A. J. F. de Almeida, S. Barreiro, W. S. Martins, R. A. de Oliveira, D. Felinto, L. Pruvost, and J. W. R. Tabosa, Opt. Lett. **40**, 2545 (2015).
5. M. Hosseini, B. Sparkes, G. Hetet, J. J. Longdell, P. K. Lam, and B. C. Buchler, Nature **461**, 241 (2009).
6. M. Afzelius, C. Simon, H. De Riedmatten, and N. Gisin, Phys. Rev. A **79**, 052329 (2009).
7. M. Saffman, T. G. Walker, and K. Mølmer, Rev. Mod. Phys. **82**, 2313 (2010).
8. Y. O. Dudin and A. Kuzmich, Science **336**, 887 (2012).
9. D. Yan, C. L. Cui, Y. M. Liu, L. J. Song, and J. H. Wu, Phys. Rev. A. **87**, 023827 (2013).
10. L. Isenhower, E. Urban, X. L. Zhang, A. T. Gill, T. Henage, T. A. Johnson, T. G. Walker, and M. Saffman, Phys. Rev. Lett. **104**, 010503 (2010).
11. S. Baur, D. Tiarks, G. Rempe, and S. Dürr, Phys. Rev. Lett. **112**, 073901 (2014).
12. H. Gorniaczyk, C. Tresp, J. Schmidt, H. Fedder, and S. Hofferberth, Phys. Rev. Lett. **113**, 053601 (2014).
13. D. Tiarks, S. Schmidt, G. Rempe, and S. Dürr, Sci. Adv. **2**, e1600036 (2016).
14. L. Allen, M. W. Beijersbergen, R. J. C. Spreeuw, and J. P. Woerdman, Phys. Rev. A **45**, 8185 (1992).
15. Z. Fang, Y. Yao, K. Xia, and J. Li, Chin. Opt. Lett. **13**, 031405 (2015).
16. S. Fu, T. Wang, Y. Gao, and C. Gao, Chin. Opt. Lett. **14**, 080501 (2016).
17. D. S. Ding, Z. Y. Zhou, B. S. Shi, and G. C. Guo, Nat. Commun. **4**, 2527 (2013).
18. A. Nicolas, L. Veissier, L. Giner, E. Giacobino, D. Maxein, and J. Laurat, Nat. Photon. **8**, 234 (2014).
19. D. S. Ding, W. Zhang, Z. Y. Zhou, J. S. Pan, G. Y. Xiang, B. S. Shi, and G. C. Guo, Phys. Rev. A **90**, 042301 (2014).
20. D. S. Ding, W. Zhang, Z. Y. Zhou, S. Shi, G. Y. Xiang, X. S. Wang, Y. K. Jiang, B. S. Shi, and G. C. Guo, Phys. Rev. Lett. **114**, 050502 (2015).
21. D. S. Ding, W. Zhang, S. Shi, Z. Y. Zhou, Y. Li, B. S. Shi, and G. C. Guo, Light Sci. Appl. **5**, e16157 (2016).
22. Z. Q. Zhou, Y. L. Hua, X. Liu, G. Chen, J. S. Xu, Y. J. Han, C. F. Li, and G. C. Guo, Phys. Rev. Lett. **115**, 070502 (2015).
23. Y. Liu, J. H. Wu, B. S. Shi, and G. C. Guo, Chin. Phys. Lett. **29**, 4205 (2012).
24. R. Pugatch, M. Shuker, O. Firstenberg, A. Ron, and N. Davidson, Phys. Rev. Lett. **98**, 203601 (2007).